MOLECULAR AND CELLULAR BIOLOGY, Oct. 2010, p. 4828–4839 Vol. 30, No. 20
0270-7306/10/$12.00 doi:10.1128/MCB.00285-10

Replication Factor C Recruits DNA Polymerase δ to Sites of Nucleotide Excision Repair but Is Not Required for PCNA Recruitment▽

René M. Overmeer,[2]† Audrey M. Gourdin,[1]† Ambra Giglia-Mari,[1,5] Hanneke Kool,[2] Adriaan B. Houtsmuller,[3] Gregg Siegal,[4] Maria I. Fousteri,[2,6] Leon H. F. Mullenders,[2]* and Wim Vermeulen[1]*

Department of Genetics, Erasmus MC, Dr. Molewaterplein 50, 3015 GE Rotterdam, Netherlands[1]; Department of Toxicogenetics, Leiden University Medical Center, 2333 RC Leiden, Netherlands[2]; Department of Pathology, Erasmus MC, Dr. Molewaterplein 50, 3015 GE Rotterdam, Netherlands[3]; Leiden Institute of Chemistry, Leiden University, Einsteinweg 55, 2300 RA Leiden, Netherlands[4]; CNRS, Institut de Pharmacologie et de Biologie Structurale, 205 route de Narbonne, F-31077 Toulouse, France[5]; and Biomedical Sciences Research Center Alexander Fleming, Vari 166-72, Greece[6]

Received 15 March 2010/Returned for modification 20 April 2010/Accepted 28 July 2010

Nucleotide excision repair (NER) operates through coordinated assembly of repair factors into pre- and postincision complexes. The postincision step of NER includes gap-filling DNA synthesis and ligation. However, the exact composition of this NER-associated DNA synthesis complex *in vivo* and the dynamic interactions of the factors involved are not well understood. Using immunofluorescence, chromatin immunoprecipitation, and live-cell protein dynamic studies, we show that replication factor C (RFC) is implicated in postincision NER in mammalian cells. Small interfering RNA-mediated knockdown of RFC impairs upstream removal of UV lesions and abrogates the downstream recruitment of DNA polymerase delta. Unexpectedly, RFC appears dispensable for PCNA recruitment yet is required for the subsequent recruitment of DNA polymerases to PCNA, indicating that RFC is essential to stably load the polymerase clamp to start DNA repair synthesis at 3′ termini. The kinetic studies are consistent with a model in which RFC exchanges dynamically at sites of repair. However, its persistent localization at stalled NER complexes suggests that RFC remains targeted to the repair complex even after loading of PCNA. We speculate that RFC associates with the downstream 5′ phosphate after loading; such interaction would prevent possible signaling events initiated by the RFC-like Rad17 and may assist in unloading of PCNA.

A multitude of endogenous and exogenous genotoxic agents induce damage to DNA. When not repaired properly, these DNA lesions can interfere with replication and transcription and thereby induce deleterious events (i.e., cell death, mutations, and genomic instability) that affect the fate of organisms (18). To ensure the maintenance of the DNA helix integrity, a network of defense mechanisms has evolved including accurate and efficient DNA repair processes. One of these processes is the nucleotide excision repair (NER) pathway that removes a wide range of DNA helix-distorting lesions, such as sunlight-induced photodimers, for example, cyclobutane pyrimidine dimers (CPD) and pyrimidine 6-4 pyrimidone photoproducts (6-4PP). Within NER, more than 30 polypeptides act coordinately, starting from the detection and removal of the lesion up to the restoration of the DNA sequence and chromatin structure. The importance of NER is underlined by the severe clinical consequences associated with inherited NER defects, causing UV-hypersensitive autosomal recessive syndromes: the cancer-predisposing xeroderma pigmentosum (XP) and the premature ageing and neurodegenerative disorders Cockayne syndrome (CS) and trichothiodystrophy (TTD) (27).

The initial DNA damage recognition step in NER involves two subpathways: transcription-coupled repair (TCR) and global genome repair (GGR). TCR is responsible for the rapid removal of transcription-blocking DNA lesions and is initiated when elongating RNA polymerase II stalls at a DNA lesion on the transcribed strand (16). In GGR, which removes lesions throughout the genome, damage recognition is facilitated by the concerted action of the heterodimeric XP group C (XPC)-HR23B protein complex and by the UV-damaged DNA-binding protein (UV-DDB) complex (10, 33). Subsequently, the 10-subunit TFIIH complex unwinds the DNA around the lesion. This partially unwound structure is stabilized by the single-strand binding protein replication protein A (RPA) and the damage-verifying protein XPA. Collectively, these proteins load and properly orient the structure-specific endonucleases XPF-ERCC1 and XPG that incise 5′ and 3′ of the damage, respectively, creating a single-strand gap of approximately 30 nucleotides (nt) (14, 40). The postincision stage of NER consists of gap-filling DNA synthesis (repair replication), ligation, and restoration of chromatin structure. These steps involve various factors that are also implicated in replicative DNA synthesis. For gap-filling synthesis the proliferating cell nuclear antigen (PCNA) is recruited and loaded onto the 3′ double-stranded DNA (dsDNA)–single-strand junction. This facili-

* Corresponding author. Mailing address for Leon H. F. Mullenders: Department of Toxicogenetics, Leiden University Medical Center, 2333 RC Leiden, Netherlands. Phone: 31 71 5269603. Fax: 31 10 5268284. E-mail: l.mullenders@lumc.nl. Mailing address for Wim Vermeulen: Department of Genetics, Erasmus MC, Dr. Molewaterplein 50, 3015 GE Rotterdam, Netherlands. Phone: 31 10 4087194. Fax: 31 10 4089468. E-mail: w.vermeulen@erasmusmc.nl.
† R.M.O. and A.M.G. contributed equally.
▽ Published ahead of print on 16 August 2010.

tates DNA synthesis by several DNA polymerases including polymerase epsilon (Polε) and polymerase delta (Polδ), the latter of which has been shown to require polymerase kappa (Polκ) for efficient repair synthesis (35). The resulting nick is sealed by either DNA ligase III/XRCC1 in quiescent cells or by both DNA ligase III/XRCC1 and DNA ligase I in dividing cells (32). Finally, chromatin assembly factor 1 (CAF-1) facilitates the restoration of the chromatin (15).

PCNA is a mobile platform for a large number of proteins involved in DNA replication and repair. In eukaryotes, PCNA forms a very stable homotrimeric ring, which must be opened to be loaded around dsDNA. During nuclear DNA replication this task is performed by replication factor C (RFC) at a primer-template junction in an ATP-dependent reaction (41, 48). RFC consists of five subunits, RFC1 to RFC5 (RFC1-5) (140, 40, 37, 38, and 36 kDa), which share a large extent of homology (46). In *in vitro* reconstituted NER assays, purified RFC was able to perform the loading of PCNA (4, 30) in a manner similar to that observed for *in vitro* replicative DNA synthesis. However, the role of RFC as the responsible clamp-loader in NER has not been proven *in vivo*. Moreover, XPG possesses PCNA binding capacity and has been implicated in the recruitment of PCNA to incised DNA (12, 30, 40). Nevertheless, the involvement of RFC in other DNA repair pathways is supported by a recent study in living cells showing that both green fluorescent protein (GFP)-tagged RFC and PCNA accumulate rapidly at sites of single- and double-strand breaks induced by UVA laser irradiation (17).

The uncertainty concerning the role of RFC in loading PCNA during NER is even further extended by the presence of other RFC-like complexes with largely unknown functions in which the four smaller subunits of RFC are associated with other proteins. First, the heteropentameric complex of Ctf18 and RFC2-5 was shown to associate with two other factors, Dcc1 and Ctf8, and is implicated in sister chromatid cohesion during mitosis (24). Interestingly, *in vitro* data show that the Ctf18 complex is able, though in an inefficient manner, to perform the loading/unloading of PCNA (38). PCNA has also been shown to interact with Elg1-RFC, another RFC-like complex (23). Little is known about this complex except that it is involved in genome stability (25). The most studied RFC-like complex in eukaryotes is the Rad17-RFC protein complex that plays an important role in the DNA damage response. *In vitro* studies reported that Rad17-RFC does not load PCNA itself but a PCNA-like sliding clamp formed by Rad9-Rad1-Hus1 (also known as 9-1-1) at 5′ termini of double- and single-stranded DNA junctions (5, 7). This loading leads to the activation of an ATR-dependent DNA damage signaling pathway and subsequent activation of cell cycle checkpoints (36).

In order to separate replication factor C from these alternative RFC-like complexes and to study its role and behavior in repair, we focused our study on the unique component, i.e., the largest subunit, or RFCp140 (RFC1). The data show that RFCp140 dynamically interacts with other NER postincision factors in a UV-dependent fashion but unexpectedly associates with the repair site even after loading PCNA, suggesting additional roles of RFC in the postincision step of NER.

MATERIALS AND METHODS

Cell lines and culture conditions. All cells were grown under standard conditions at 37°C and 5% CO_2; simian virus 40 (SV40)-immortalized fibroblasts, MRC5 (wild type), C5ROhtert-GFP-hPCNA cells (9), and XPCS2BA (XPB) cells transfected with pEGFP were grown in a 1:1 mixture of Ham's F-10 medium and Dulbecco's modified Eagle's medium (DMEM) supplemented with 10% fetal calf serum (FCS) and 1% penicillin-streptomycin (PS). Human diploid primary fibroblasts or human telomerase reverse transcriptase (hTERT)-immortalized fibroblasts derived from a healthy individual (VH10 cells) or from NER patients (XP25RO, XP21RO, XP51RO and XPCS1RO, corresponding to XP group A, C, F, and G cells, respectively), and human quasi-diploid bladder carcinoma cells (EJ30) were grown on DMEM with 10% FCS and 1% PS. G418 (600 μg/ml) was added as a selection marker where appropriate. To study quiescent cells, the cells were grown to confluence and subsequently incubated for 5 days with medium containing 0.2% FCS.

Global and local UV irradiation. Prior to (confocal) microscopy and immunofluorescence experiments, cells were seeded on 24-mm coverslips (Menzol), coated with Alcian blue (Fluka), rinsed with phosphate-buffered saline (PBS), and irradiated with a Philips TUV lamp (predominantly 254 nm). After irradiation cells were incubated with their original medium before being processed for microscopy experiments or immunofluorescence. For local irradiation cells were covered with a microporous polycarbonate filter containing 3-, 5-, or 8-μm pores (Millipore, Bradford, MA) as previously described (31, 45). For living-cell studies, the UV doses were as follows: for cells irradiated with a lamp through the filter, the UV dose induced was 120 J/m^2; for cells treated with hydroxyurea/cytosine-β-arabinofuranoside (HU/Ara-C), the irradiation dose was 30 J/m^2; for the UVC laser, the scanning time was 500 ms.

Immunofluorescence. Experiments were performed as described previously (32). All immunofluorescence experiments were performed using hTERT-immortalized cells, with the exception of XPF cells, which were primary. Prior to fixation cells were kept on ice and washed with PBS. If required, PBS–0.2% Triton X-100 (Triton wash) was added to the cells for 5 min. Cells were fixed and permeabilized by adding PBS containing 2% paraformaldehyde for 10 min, followed by a 5-min incubation in 0.2% Triton X-100. After fixation and permeabilization, slides were washed with PBS and blocked with 3% BSA in PBS for 30 min. Slides were incubated with primary and secondary antibodies diluted in PBS containing 0.5% BSA–0.05% Tween 20 for 2 h and 1 h at room temperature, respectively, with 1.5 μg/ml 4′,6′-diamidino-2-phenylindole (DAPI) added to the secondary antibody solution. After each antibody the slides were washed three times with PBS–0.05% Tween 20. Slides were then mounted with Polymount (Polysciences Inc., Warrington, PA). For the competition experiments, hydroxyurea (Fluka) and cytosine-β-arabinofuranoside were added to the medium 30 min prior to the first irradiation, with final concentrations of 10 mM and 100 μM, respectively.

6-4PP repair analysis. To measure 6-4PP repair, cells were treated as described above and irradiated with 15 J/m^2 of UVC. After 1, 2, 4, or 8 h of repair, cells were fixed and stained for the presence of 6-4PP using 6-4PP-recognizing antibodies (see below). Microscopy settings used for quantification of fluorescent signal have been described previously (33). In short, images were taken with equal exposure times, and the total fluorescence per nuclei was measured for 50 to 100 nuclei per point per experiment (Axiovision software). Graphs represent the average of four independent experiments.

Quantitative spot analysis. To quantify spot incidence and intensity, cells were locally irradiated (8 μm) with 30 J/m^2 and stained for XPA and PCNA or XPA and Polδ. Spot incidence was measured by manually scoring >100 cells containing XPA local UVC damage (LUD) for colocalization of PCNA or Polδ. Spot intensity was measured by making images with identical exposure settings. Subsequently, the XPA LUD was used to define the spot area and the XPA, PCNA, or Polδ average signal intensity within the spot was measured (Axiovision software). Cells scored negative for PCNA or Polδ spot incidences were excluded from further analysis. The average spot intensities of >100 cells were measured for each point.

Antibodies. Primary antibodies were rabbit polyclonal anti-PCNA (Ab2426; Abcam), mouse monoclonal anti-PCNA (PC10 Ab29; Abcam and Dako), anti-GFP (clone 7.1 and 13.1, Roche), anti-DNA Polδ (Abcam), anti-RPA (Abcam), anti-XRCC1 (Santa Cruz), anti-6-4PP dimer (clone 64 M-2; Cosmo Bio), rabbit polyclonal anti-p89 (Santa Cruz), anti-RFC5 (Abcam), anti-Ki67 (Ab16667; Abcam), anti-DNA Polδ (Santa Cruz), and goat polyclonal anti-RFC1 (Ab3566; Abcam). Mouse monoclonal anti-RFC1 was a kind gift of B. Stillman, Cold Spring Harbor Laboratory, and rabbit polyclonal anti-Lig1 was a gift from A. E. Tomkinson, University of Baltimore, Baltimore, MD. Whereas mouse monoclo-

nal anti-RFC1 was used for immunofluorescence, goat polyclonal anti-RFC1 was used for Western analysis.

Secondary antibodies for immunofluorescence staining were Cy3-conjugated goat anti-mouse antibody, Cy3-conjugated goat anti-rabbit IgG and fluorescein isothiocyanate (FITC)-conjugated donkey anti-mouse antibody (Jackson Immuno-Research Laboratories), Alexa Fluor 488-conjugated goat anti-mouse IgG, Alexa Fluor 488-conjugated goat anti-rabbit antibody, and Alexa Fluor 555-conjugated goat anti-rabbit antibody (Molecular Probes). For Western blotting, the following were used: horseradish peroxidase (HRP)-coupled polyclonal rabbit anti-mouse and polyclonal donkey anti-rabbit (DakoCytomation), IR700-coupled donkey anti-goat and donkey anti-rabbit, and IR800-coupled donkey anti-mouse antibodies. All secondary antibodies were used according to the manufacturer's instructions.

Subcellular fractionation and immunoprecipitation. For coimmunoprecipitation (co-IP) studies, non-cross-linked cells were fractionated by adaptation of an Abcam protocol (1). After trypsinization and a PBS wash, cells were resuspended in 10 mM HEPES (pH 7.9), 1.5 mM $MgCl_2$, 10 mM KCl, 0.5 mM dithiothreitol (DTT), and 0.05% NP-40 (or Igepal) and left on ice for 10 min and centrifuged at 3,000 rpm for 10 min at 4°C. The pellet was resuspended in 5 mM HEPES (pH 7.9), 1.5 mM $MgCl_2$, 0.2 mM EDTA, 0.5 mM DTT, and 26% glycerol (vol/vol) and supplemented with 5 M NaCl to a final concentration of 400 mM. The solution was homogenized by pipetting 20 times through a 200-μl fine tip and kept for 1 h on ice. The supernatant (soluble fraction) was aliquoted after being spun for 60 min at 13,200 rpm at 4°C. The pellet (chromatin fraction) was dissolved in SDS sample buffer.

Co-IP reactions were performed in binding buffer (20 mM HEPES-KOH [pH 7.8], 1 mM EDTA, 0.5 mM EGTA, 0.15 M NaCl, 10% glycerol, 0.1% Triton X-100, 1 mM phenylmethylsulfonyl fluoride [PMSF], and a mixture of protein-ase/phosphatase inhibitors) overnight at 4°C. For each reaction, 400 mg of nuclear extract was immunoprecipitated with 0.5 to 3 μg of antibody. Immunocomplexes were then collected by adsorption for 1 h at 4°C to precleared protein A or G beads (Upstate). The beads/immunocomplexes were subsequently washed five times with 20 bed volumes of binding buffer containing 300 mM NaCl and 0.5% Triton X-100. Finally, they were resuspended in 1 bed volume of SDS sample buffer, incubated for 10 min at 95°C, and analyzed by Western blotting.

ChIP. *In vivo* cross-linking and chromatin immunoprecipitation (ChIP) were performed as described previously (11). Briefly, human quasi-diploid bladder carcinoma cells (EJ30 cells) were incubated for 40 min after UV irradiation (time corresponding to a maximal amount of NER complexes). Cells were cross-linked at 4°C with 1% formaldehyde buffer and lysed, and chromatin was purified and fractionated. For each ChIP reaction, an equal amount of cross-linked chromatin extract was added to the mixture and incubated overnight in 1× radioimmunoprecipitation assay (RIPA) buffer with 0.5 to 3 μg of a specific antibody. Antibody complexes were bound by adding precleared protein A or G beads (Upstate). The supernatant (unbound fraction) was kept, and the beads were washed for a total of six times with increasing stringency. Antibody and bound complexes were then eluted by boiling the beads in 1 bed volume of 2× Laemmli SDS sample buffer for 30 min to 1 h at 95°C, which reversed the cross-linking, and analyzed by SDS-PAGE. Coprecipitating proteins were analyzed by Western blotting.

Knockdown of RFCp140. A total of 10^6 of hTERT-immortalized fibroblasts were seeded per p90 dish, followed by three rounds of transfection with HiPerfect and control RNA (small interfering RNA [siRNA] directed against GFP [siGPF] or siRFC; Smartpool, Dharmacon) (see reference 35 for details) at 24 h, 48 h, and 96 h after seeding. Experiments were done 72 h after the last transfection.

Confocal microscopy. (i) Live-cell microscopy. Confocal images of the cells were obtained using a Zeiss LSM 510 microscope equipped with a 25-mW Ar laser at 488 nm and a 40×, 1.3-numerical aperture (NA) oil immersion lens. GFP fluorescence was detected using a dichroic beam splitter (HFT 488), a beam splitter (NFT 490), and an additional 505- to 550-nm band-pass emission filter.

(ii) Fixed cells. For images of cells after immunofluorescence, the 25-mW Ar laser at 488 nm together with a He/Ne 543-nm laser, and a 40×, 1.3-NA oil immersion lens were used. Alexa Fluor 488 was detected using a dichroic beam splitter (HFT 488) and an additional 505- to 530-nm band-pass emission filter. Cy3 was detected using a dichroic beam splitter (HFT 488/543) and a 560- to 615-nm band-pass emission filter.

Photobleaching procedures. (i) Half-nucleus bleaching combined with FLIP-FRAP. Data analysis was performed in the following way (schematically illustrated in Fig. 5): the fluorescence recovery (FRAP) in the bleached area was subtracted from the fluorescence loss (FLIP) in the nonbleached part of the nucleus. The difference in fluorescence signal between the FLIP and FRAP areas before bleaching was set at 0, and the difference in fluorescence between the FLIP and FRAP areas after bleaching was normalized to 1 and plotted against the time after bleaching. The mobility of the protein was determined as the time necessary for FLIP-FRAP to return to 0 (i.e., the time required to reach full redistribution of bleached and nonbleached molecules).

(ii) FRAP in local damage. The entire local damage was bleached in 1.2 s by two bleaching pulses, and the recovery of fluorescence was monitored for 60 s by scanning the whole cell every 5 s. To overcome the variability in the size and intensity of the damage (i.e., the number of proteins immobilized), the curve was normalized to the overall fluorescence in the cell (including the local damage itself).

RESULTS

Involvement of replication factor C in nucleotide excision repair *in vivo*. To investigate the involvement of RFC in NER, we assessed the subcellular distribution of endogenous mammalian RFC in quiescent human fibroblasts following induction of local UVC damage (LUD) through a microporous filter (31, 45). As RFC also plays a role in replication and likely in other replication-associated strategies to overcome DNA damage-induced replication blockage (such as translesion synthesis or recombination), the analysis in quiescent cells is crucial to investigate its possible function in NER. Immunofluorescence analysis using an antibody against RFCp140 revealed that RFC is recruited to the LUD and colocalizes with other NER core factors, such as the TFIIH complex subunit p89 (Fig. 1A) and replication-associated postincision NER factors such as PCNA (Fig. 1C). The recruitment of RFC to LUD is dependent on active NER as RFC binding is severely impaired in NER-deficient cell strains carrying mutations in upstream factors such as XPA, XPF, or XPG (Fig. 1A).

Previously, we found that ligation of the repair patch in NER involves different DNA ligases depending on the proliferative status of the cell, i.e., ligase III/XRCC1 in quiescent cells and both ligase I and ligase III/XRCC1 in proliferating cells (32). Since RFC is also an essential replication factor differentially regulated in proliferating cells (43), we investigated whether RFC loading to LUD depends on the proliferation status of the cell. As shown in the top panel of Fig. 1B, RFCp140 is bound to LUD in both proliferating (Ki67 marker positive) and in quiescent cells. This proliferation-independent RFC recruitment is confirmed by costaining with ligase I; i.e., RFCp140 accumulates at LUD in cells lacking ligase I and in cells having ligase I present at LUD.

Surprisingly, in virtually all cells both PCNA and RFCp140 were already visible at LUD shortly (<5 min) after damage infliction, similar to the preincision factor TFIIH (p89) (Fig. 1C). Please note that this does not imply that the postincision factors are loaded simultaneously with preincision factors as this analysis is not suited to determine actual assembly kinetics. In previous work we showed that the assembly of preincision precedes the loading of the postincision factors (29). Four hours after UV irradiation, localization of TFIIH to LUD is strongly reduced compared to that at earlier time points and almost undetectable 8 h after UV-exposure, following the kinetics of 6-4PP removal (44). In contrast, RFC and PCNA remain clearly visible at LUD up to 8 h after exposure. These data suggest that the release of factors involved in the postincision stage of NER is much slower than the actual damage removal and gap-filling synthesis step. Strikingly, although

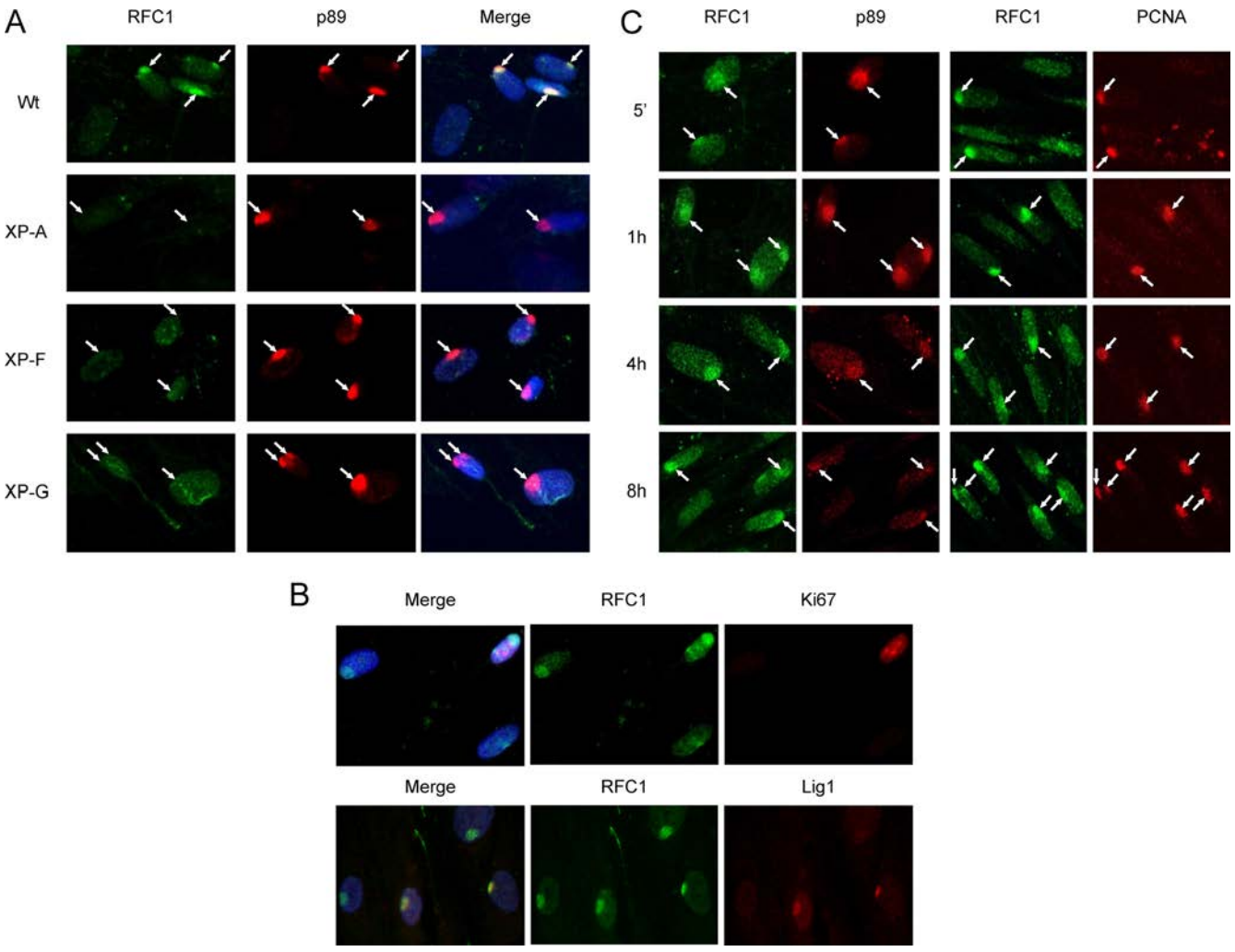

FIG. 1. RFCp140 localizes to sites of damage in an NER-dependent and cell cycle-independent manner. Primary and hTERT-immortalized cells were grown to confluence prior to UV irradiation. (A) Immunofluorescent staining of RFCp140 (RFC1) and TFIIH subunit p89 in normal and NER-deficient human fibroblasts. Wt, wild type. (B) Costaining of RFCp140 and proliferation marker Ki67 (top panel) or ligase I (lower panel) in normal human fibroblasts. (C) Kinetics of RFCp140 localization at sites of damage over time compared to preincision factor p89 (left) and postincision factor PCNA (right). Arrows point to position of the LUD.

RFC is supposed to function as PCNA loader, these data argue for a role beyond simply loading of PCNA.

UV-induced binding of RFC to chromatin and NER postincision factors. To further investigate the involvement of RFC in NER-induced repair replication, we isolated NER complexes actively engaged in the repair process by *in vivo* formaldehyde cross-linking of UV-irradiated cells, isolation of chromatin fragments (300 to 600 bp), and chromatin immunoprecipitation (ChIP) (11). Subsequently, candidate NER proteins that were expected to be coprecipitated were analyzed by Western blotting. For this purpose, confluent cells were irradiated with 20 J/m^2 of UVC, creating an average of 1 photolesion (CPD or 6-4PP) every 2.5 kb of dsDNA (11), ensuring that the vast majority of the purified chromatin fragments contained no more than a single repair complex. RFCp140-specific ChIP revealed a UV-induced coprecipitation of RPA, PCNA, and Polδ (Fig. 2A). Strikingly, no increase of the preincision factor p89 was observed, further corroborat-

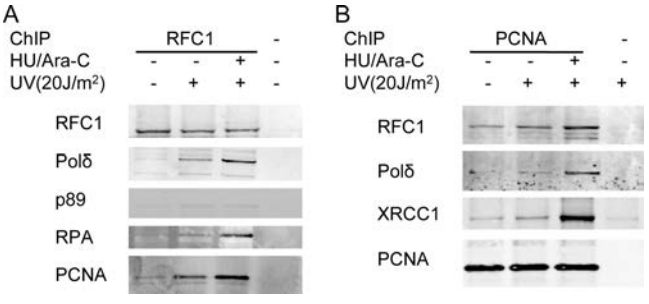

FIG. 2. UV-dependent association of RFCp140 (RFC1) with postincision complexes. Serum-starved EJ30 cells were irradiated with 20 J/m^2 1 h prior to formaldehyde cross-linking. Subsequent ChIP was performed with goat anti-RFCp140 (A) and mouse anti-PCNA (B). In both panels, no antibody was added to the far-right lanes. Precipitated proteins were analyzed by Western blotting as indicated.

ing that the pre- and postincision NER stages are temporally separable events. A reciprocal experiment using ChIP against PCNA revealed a clear UV-dependent increase of the postincision NER factors XRCC1 and RFCp140 (Fig. 2B). Inhibition of gap-filling synthesis significantly increased the amount of coprecipitating replication factors, including Polδ. In particular, coprecipitation of RPA was only marginally increased after UV irradiation but significantly increased after synthesis inhibition. Such an increase in interaction is likely due to the accumulation of incomplete gap-filling complexes (R. M. Overmeer, unpublished data). These data confirm the role of RFC in repair of UV lesions and suggest that RFC remains involved in the postincision complex after loading PCNA.

The accumulation of both p89 and RFCp140 at LUD shortly after local UV exposure (5 min) (Fig. 1C) seems to contradict the two temporally separable complexes identified by ChIP (Fig. 2). However, a single LUD site contains numerous photolesions with various repair complexes in different phases of the repair process; as such, immunofluorescence studies reveal an ensemble of multiple dynamic repair complexes and are not suited to dissect temporal stages of NER. In contrast, ChIP analysis deals with chromatin fragments that encompass, on average, a single repair complex, thereby allowing accurate determination of the composition of RFCp140-containing complexes.

RFC1 is required for loading but not for recruitment of PCNA to NER sites. Having shown that RFCp140 is involved in NER-associated repair replication, we further analyzed the consequences of depleting RFCp140 for the different stages of the NER reaction. To that aim we performed siRNA-mediated knockdown of RFCp140 in high-density seeded cells, resulting in approximately 90% knockdown when cells reached confluence (Fig. 3A).

Knockdown of RFCp140 resulted in inhibition of DNA damage removal in a fashion reminiscent of that seen when repair synthesis is inhibited by HU and Ara-C, thereby confirming the requirement for RFCp140 for efficient NER (Fig. 3C) (32; also Overmeer, unpublished). Interestingly, when we analyzed the colocalization of Polδ with XPA at LUD in cells treated with siRNA against RFCp140, approximately half of the cells showed no Polδ at sites of damage marked by XPA accumulation (Fig. 3D and F), whereas control siRNA-treated cells displayed >99% colocalization. This reduced colocalization was not due to a spurious remaining fraction of RFCp140 bound to chromatin after the siRNA as cellular fractionation showed that RFCp140 was depleted from both the soluble and chromatin-bound pools (Fig. 3B). In contrast, knockdown of RFCp140 had no significant effect on the recruitment of PCNA to sites of UV damage (Fig. 3E and F). This surprising result suggests that RFCp140 is not required for the recruitment of PCNA to NER sites but is needed to recruit and/or stably load Polδ.

Semiquantitative measurement of the average spot intensity of proteins at LUD sites in cells treated with siRNA against RFCp140 revealed enhanced intensities of accumulation for XPA (Fig. 3D, E, and F), compared to cells treated with control siRNA. Impaired gap filling in cells treated with siRNA against RFCp140 might underlie the enhanced XPA intensity as similarly enhanced XPA intensity at LUD sites was observed in cells when gap filling was abolished by treatment with the DNA synthesis inhibitors HU and Ara-C (39) (Fig. 3F).

The reduced amount of Polδ, together with a reduced spot incidence of Polδ (relative to XPA) at LUD after knockdown of RFCp140 (Fig. 3E and F), further corroborates the suggestion that in the absence of RFC, Polδ is not efficiently recruited to repair sites. In contrast to repair inhibition by RFCp140 knockdown, inhibition of repair synthesis by HU and Ara-C caused increased signals of PCNA and Polδ (confirming the ChIP data shown in Fig. 2). This is expected as all postincision NER factors are properly loaded in the presence of chemical inhibitors (Overmeer, unpublished), and repair synthesis (or UV-induced unscheduled DNA synthesis [UDS]) is initiated but not finished (34, 39), thereby generating substrate for these factors to bind. The slight decrease in PCNA spot intensity at LUD after RFCp140 knockdown might imply that although PCNA is recruited, it is improperly loaded and might easily dissociate, resulting in a decreased signal. Thus, although RFC is not required for recruitment of PCNA, it is necessary for stable association to 3′ termini and subsequent loading of Polδ.

The data demonstrate that both depletion of RFCp140 and chemical interference with replication affect the postincision NER step, although with variable consequences for the resulting accumulation of repair intermediates. However, the consequences for repair synthesis were similar as we recently found that RFCp140 depletion caused a 50% reduction of UDS (35). Previously, we showed that inhibition of repair patch ligation led to a surprising concomitant reduction in actual damage removal (32). Similarly, we observed reduced damage removal both after depletion of RFCp140 and after HU/Ara-C treatment (Fig. 3B).

Association of RFCp140-GFP with sites of replication and repair. The extended accumulation of RFC (Fig. 1C) and other postincision factors at LUD sites compared to preincision factors (e.g., p89 of TFIIH) (Fig. 1C) reflects either slow dissociation kinetics of postincision factors or additional functions of these factors beyond repair replication. To investigate the dynamics of RFC association with sites of repair, a human cell line (SV40-transformed MRC5 fibroblasts) that stably expresses RFCp140 tagged with green fluorescent protein (GFP) was generated. To prevent disturbed population growth features due to overexpression of RFCp140-GFP (13, 21, 43), we carefully checked the expression level of RFCp140-GFP and cellular growth. Immunoblot analysis of cells expressing RFCp140-GFP with an anti-RFCp140 antibody showed that endogenous RFCp140 and RFCp140-GFP were expressed at similar levels (Fig. 4D). Hybridization with anti-GFP antibodies revealed no RFCp140-GFP breakdown products, indicating that the majority of fluorescence observed in the cells is derived from the full-length fusion protein (data not shown). Moreover, the presence of RFCp140-GFP in the cells did not affect cellular growth, nor did it interfere with DNA replication, as revealed by fluorescence-activated cell sorting (FACS) analysis; UV-induced cytotoxicity (UV survival) was not enhanced, suggesting efficient repair of UV photolesions (data not shown). Immunoprecipitation of nuclear extracts with an antibody directed against one of the other RFC subunits (RFCp36) precipitated similar amounts of endogenous RFCp140 and RFCp140-GFP (Fig. 4E). These findings demonstrate that the GFP tag does not disrupt the ability of RFCp140-GFP to form a complex with the smaller RFC sub-

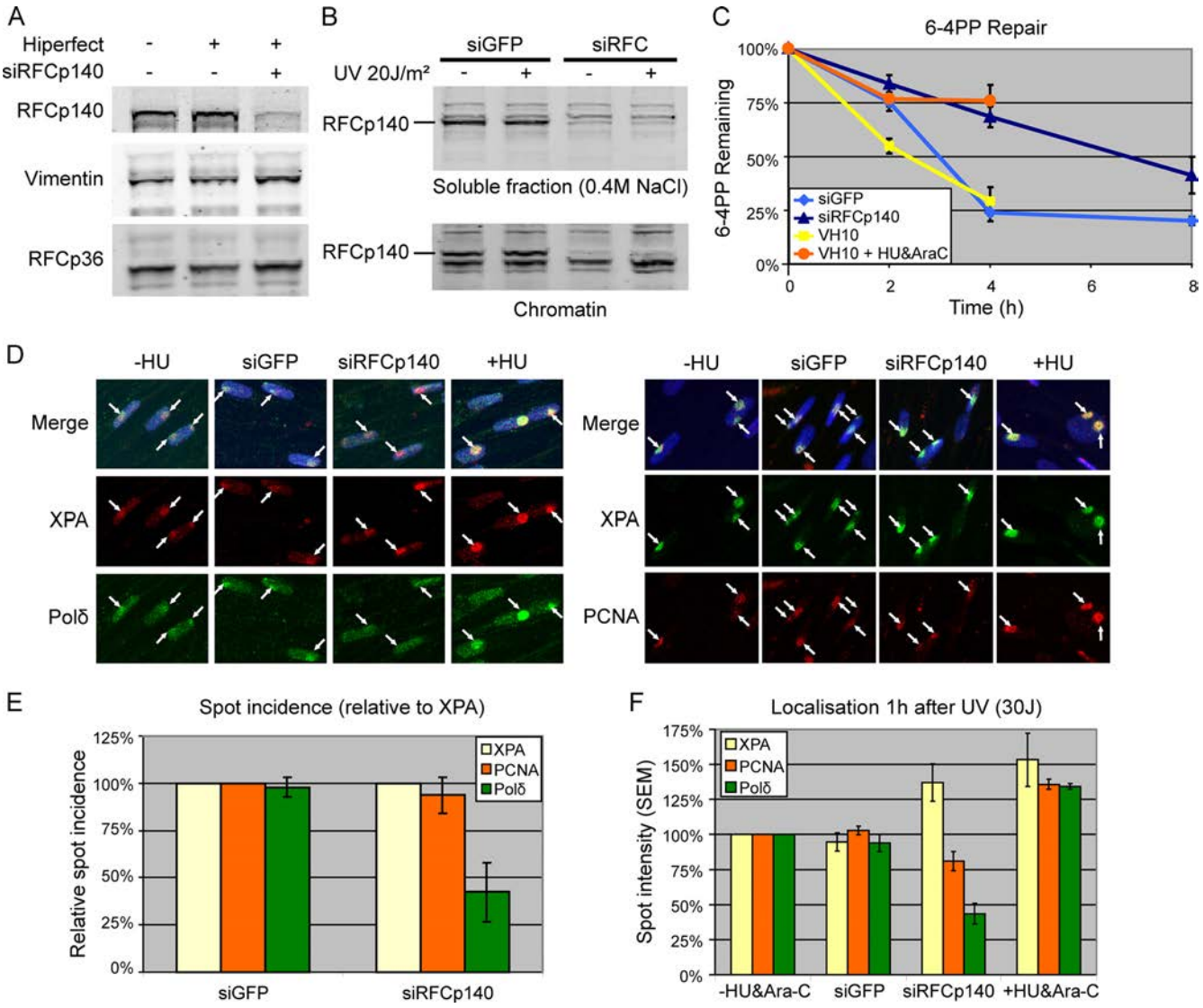

FIG. 3. Knockdown (KD) of RFCp140 inhibits efficient NER through impaired Polδ recruitment. (A) Western blot analysis of RFCp140 KD in hTERT-immortalized VH10 cells, with vimentin as a loading control. Specific KD of RFC was confirmed by staining with an RFC5-specific antibody. (B) Subcellular fractionation and subsequent Western blot analysis show that RFCp140 is depleted from both the nuclear soluble fraction and from the chromatin fraction. (C) Immunohistochemical analysis of 6-4PP repair in cells treated with siRNAs against GFP or RFCp140. Graph represents the average of four independent experiments. (D) Immunofluorescent staining of Polδ and XPA (left) or PCNA and XPA (right) in cells after mock treatment (−HU) or after treatment with siGFP, siRFCp140, or HU and Ara-C (+HU). (E) Relative percentage of visible accumulation of proteins at LUD after treatment with siRNA; LUD marked by XPA accumulation is expressed as a percentage of colocalization with XPA set at 100%. (F) Average intensity of proteins accumulated at site of LUD scored in panel C. Cells were treated and stained simultaneously, pictures were taken with identical exposure times, and the average pixel intensity for each positively scored LUD site (i.e., LUD sites scored negative in panel C were excluded) was calculated by measuring the total signal and area of each LUD site. Subsequently the average intensity was calculated and normalized to that found in nontreated cells. SEM, standard error of the mean.

units, which is necessary for the protein to fulfill its function in replication and repair.

RFCp140-GFP is localized in the nucleus; however, its distribution changes during the cell cycle. While it is homogeneous in G_1/G_2, it presents a specific, PCNA-like focal pattern during S phase (Fig. 4A). Cotransfection of cells with PCNA-mCherry shows that both proteins colocalize at these foci, which correspond to replication sites (28; also data not shown). After local UV damage infliction in cells expressing RFCp140-GFP, a clear localization to the damaged area could be observed in virtually all cells within a few minutes after irradiation (Fig. 4B, white arrows). RFCp140-GFP colocalized with PCNA-mCherry at the damaged sites, indicative of association of both proteins to NER sites (Fig. 4C, white arrows). These findings further suggest that GFP-tagged RFCp140 is targeted to activity sites (replication and repair) in a manner similar to endogenous RFCp140. Together, these data suggest that the fusion protein is expressed at physiologically relevant levels, is functional in replication and NER, and is a bona fide platform to perform live-cell protein dynamic analysis.

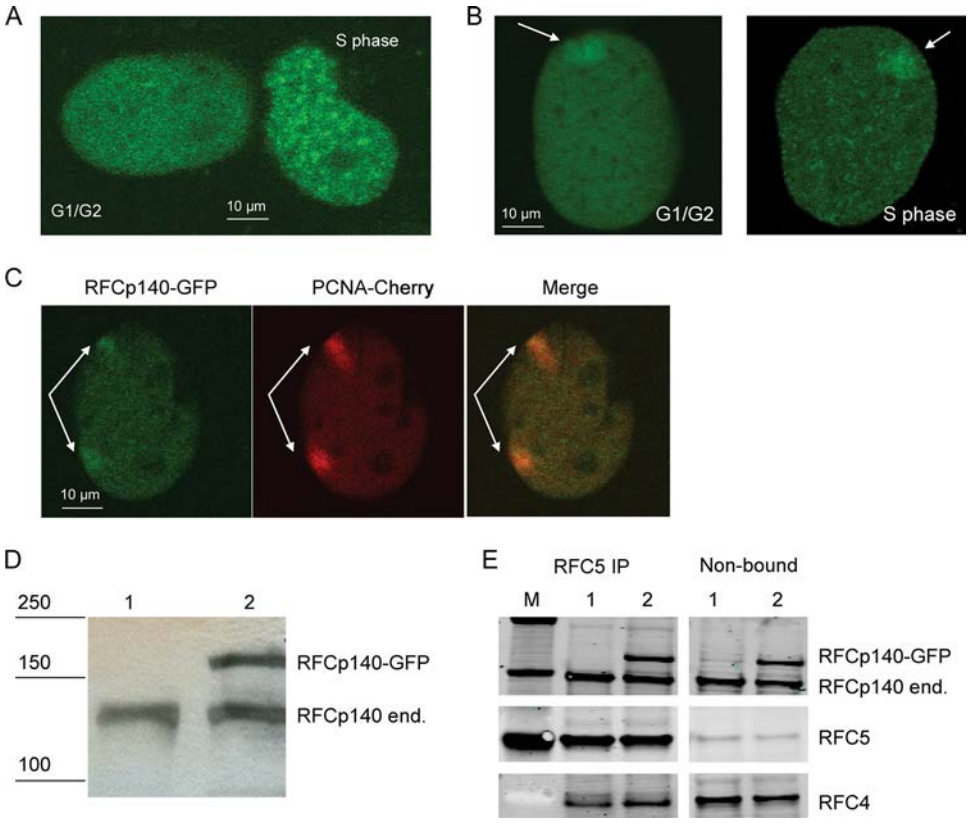

FIG. 4. GFP-RFCp140 colocalizes with PCNA-mCherry to sites of replication and to sites of repair independent of cell cycle. (A) Characteristic nuclear distribution patterns of RFCp140 seen in S-phase and non-S-phase cells. (B) Recruitment of RFCp140-GFP to sites of damage is independent of the cell cycle as it is detectable in G_1/G_2 cells and in S-phase cells. (C) Colocalization of RFCp140-GFP (left) with PCNA-Cherry (middle) at sites of damage; the right panel is the merged image. (D) Immunoblot analysis of MRC5 cells (lane 1) and MRC5 cells expressing RFCp140-GFP (lane 2), probed with anti-RFCp140, showed that the transgene produces a protein of the expected size and that RFCp140-GFP is expressed to a similar level as the endogenous (end) RFCp140. (E) RFCp346 (RFC5) was immunoprecipitated from nuclear extracts of MRC5 (lane 1) and MRC5-RFCp140-GFP (lane 2) cells, and coprecipitating proteins were analyzed by Western blotting. RFCp346 coprecipitates similar amounts of endogenous RFC4 and RFCp140 as well as with GFP-RFCp140, implying that they can form the RFC complex with similar efficiencies. Lane M, molecular mass marker (Biorad), representing (from top to bottom) 205 kDa, 150 kDa, and 37 kDa.

Dynamics of RFCp140-GFP at sites of NER. To measure the dynamic associations of RFCp140-GFP in replication and NER, protein mobility was evaluated by different photobleaching procedures. We designed an adapted FRAP (fluorescence recovery after photobleaching) protocol and combined it with a FLIP (fluorescence loss in photobleaching) protocol by bleaching the GFP fluorescence in half the nucleus and subsequently measuring the fluorescence recovery in the bleached area (recovery or FRAP) and in the nonbleached area (FLIP), as illustrated in Fig. 5A. The time required to reach an equilibrium between FRAP and FLIP is a measure of the overall nuclear mobility of RFCp140-GFP.

We first determined the mobility of RFCp140-GFP in unchallenged G_1/G_2-phase cells (recognizable by the homogenous nuclear distribution) and observed a redistribution time of approximately 120 s (Fig. 5A), significantly slower than GFP-PCNA (50 s for complete fluorescence redistribution) (Fig. 5A). To test whether the slow mobility of RFCp140-GFP is derived from transient macromolecular interactions, a temperature shift of 10°C (from 37°C to 27°C) was applied to the cells. At the lower temperature, the mobility of proteins involved in enzymatic reactions or interactions (protein/protein or protein/DNA) is reduced (19, 42). The mobility of RFCp140-GFP was unchanged, suggesting that RFCp140-GFP is freely diffusing throughout the nucleus during the G_1/G_2 phase of the cell cycle (Fig. 5B), as was previously found for GFP-PCNA (9). The slower mobility observed for RFCp140 is likely due to the larger molecular size of the RFC complex (the RFC complex, including RFCp140 and RFC2-5, has a molecular mass of 289 kDa, while trimeric PCNA-GFP is only 115 kDa) and its different shape, e.g., elongated rather than the compact globular shape of the PCNA trimer. In contrast, the mobility of RFCp140-GFP in S-phase cells (identified by the presence of foci) was sensitive to temperature: at lower temperatures the mobility is retarded. This suggests that RFCp140-GFP is transiently bound to S-phase-specific structures, likely replication foci, in a temperature-dependent fashion. Note that in S-phase cells cultured at 37°C, we do not observe an overall slower mobility than in non-S-phase cells despite the presence of higher concentrations of RFCp140-GFP at replication foci. The transient binding of RFCp140 to replication foci is apparently too short to reveal a significant mobility shift with the applied FRAP procedures unless reac-

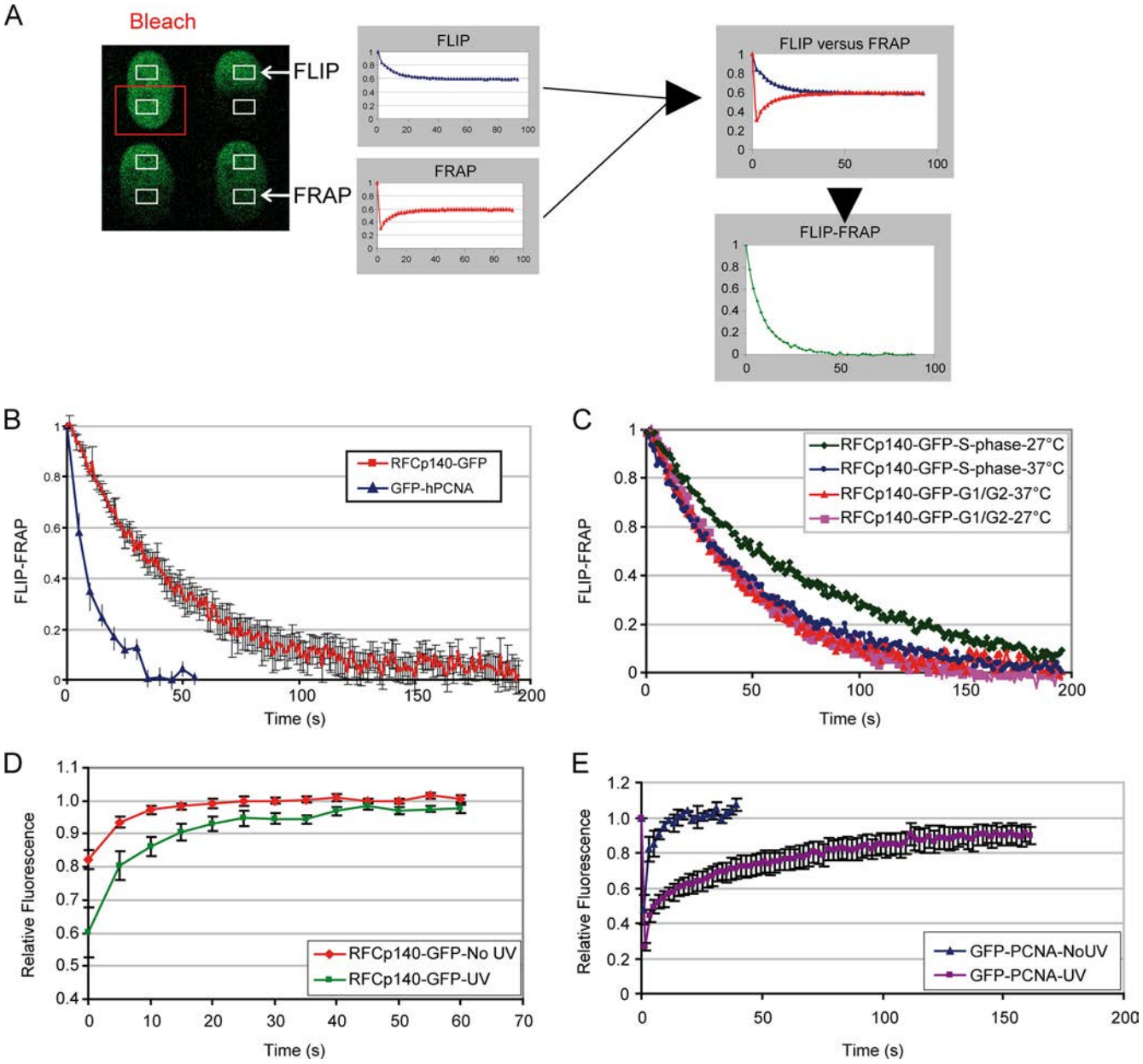

FIG. 5. FRAP analysis of the mobility of RFCp140-GFP in comparison to that of GFP-PCNA. (A) Schematic overview of the combined FLIP-FRAP analysis procedure. Half of the nucleus (indicated by the red box) is bleached by high-intensity laser excitation; the loss of fluorescence (FLIP) in the unbleached part (measured in the upper white box) is measured over time and plotted (upper left graph). The recovery of fluorescence (FRAP) in the bleached part of the cell (lower white box) is also plotted (lower left graph). The difference between FLIP and FRAP (upper right) is normalized to 1 directly after the bleach pulse and plotted over time, indicated in seconds (lower right). (B) Combined FLIP-FRAP analysis of RFCp140-GFP and GFP-PCNA in untreated cells at 37°C. (C) FLIP-FRAP analysis of RFCp140-GFP in G_1/G_2 and S-phase cells at 37°C and 27°C. (D) FRAP in a subnuclear area (similar size as LUD) of RFCp140-GFP in cells without LUD (No-UV) and in LUD (UV) (120 J/m^2); the recovery of fluorescence (expressed as relative fluorescence, where prebleach is set at 1) is plotted against time (in seconds) after bleaching. (E) FRAP of GFP-PCNA in control cells and in LUD, as in panel D.

tion kinetics or thermodynamic interactions are influenced by a temperature drop.

In order to determine the average residence or binding time of RFCp140-GFP in NER complexes, we bleached the local damage and subsequently monitored the recovery of fluorescence (20) and compared the recovery time to that of an equally sized subnuclear area of mock-treated cells. In untreated cells it took approximately 25 s for complete recovery while in damaged cells equilibrium was reached after 45 s (Fig. 5C). This rather moderate increase in residence time of RFCp140-GFP in LUD suggests a very short binding at NER sites. Surprisingly, and in contrast to the higher mobility rate of PCNA in unchallenged non-S-phase cells, not all PCNA molecules at LUD sites exchanged even 160 s after bleaching (Fig. 5D) (9). This remarkable difference in asso-

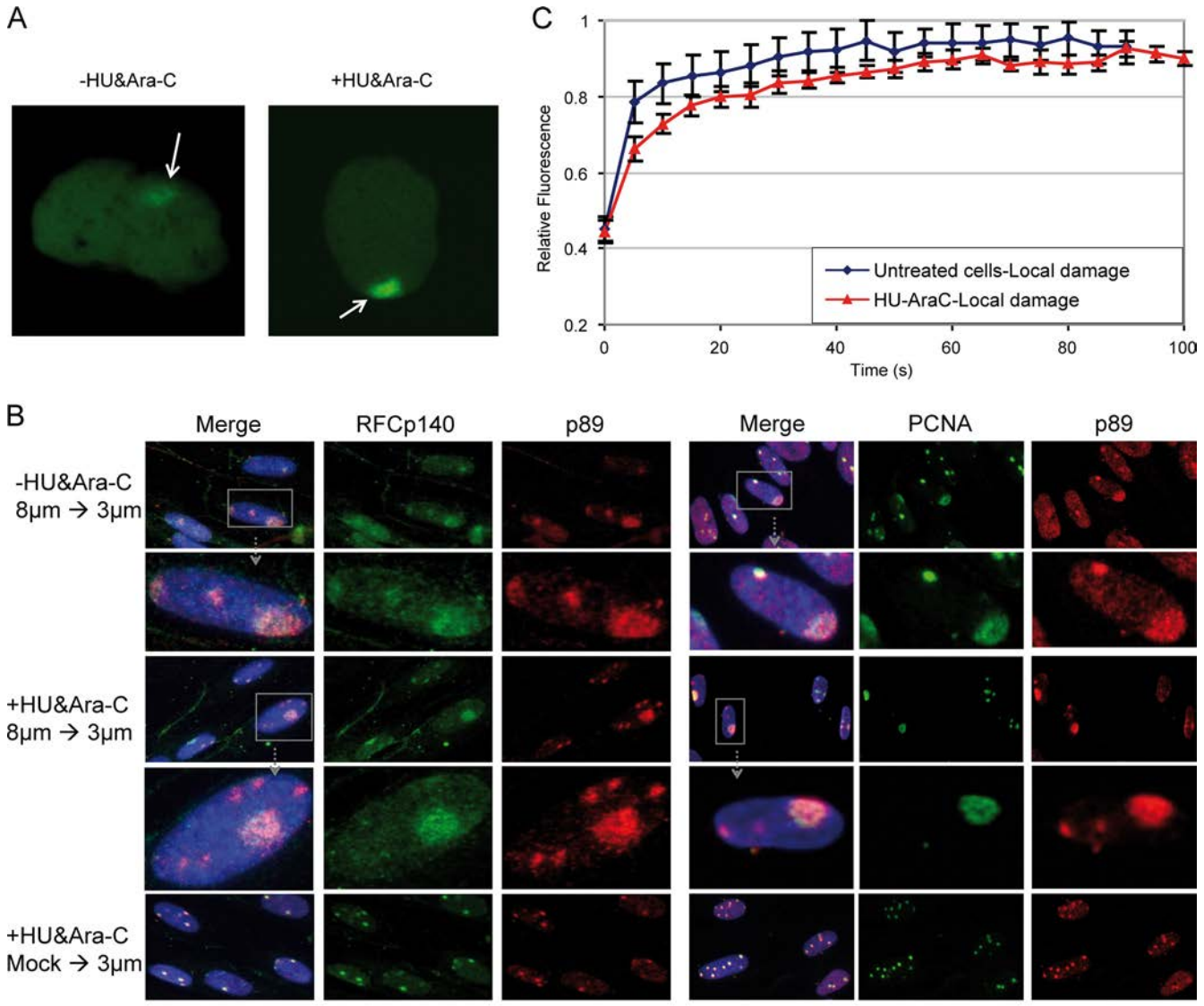

FIG. 6. (A) Confocal images of MRC5 cells expressing RFCp140-GFP after local damage (120 J/m^2), in the absence and presence of HU/Ara-C. (B) Endogenous RFCp140 and PCNA remain associated with the initial site of damage when repair synthesis is inhibited. Cells were locally irradiated through microporous filters, first with 8- and then with 3-μm pores, in the absence or presence of HU and Ara-C. Boxed cells are enlarged in the frame immediately below. (C) FRAP analysis of RFCp140-GFP in LUD in the absence and presence of HU/Ara-C.

ciation dynamics suggests a scenario in which RFCp140 continuously binds to and dissociates from NER-replication sites as long as gap filling is not completed. The relatively long residence time of PCNA suggests that the loading of PCNA to active sites is much less transient.

Stability of NER complexes in the presence of DNA synthesis inhibitors. To further decipher the function of RFC in NER, we blocked repair synthesis by addition of hydroxyurea (HU) and cytosine-ß-arabinofuranoside (Ara-C). In the presence of these inhibitors a limited number of incisions occur while PCNA and Polδ are still loaded onto DNA at NER sites; however, repair synthesis is severely reduced, repair patches remain unligated, and removal of photolesions is severely impaired (32, 34, 39).

After 30 min of incubation in the presence of these inhibitors, cells expressing RFCp140-GFP were locally irradiated, and 1 h after irradiation they were subjected to imaging, photobleaching, or fixation. Irradiated cells not treated with inhibitors were taken as a control. In the presence of DNA synthesis inhibitors, we observed a much brighter accumulation of RFCp140-GFP at local damage than in the absence of inhibitors (Fig. 6A), suggesting that under these conditions postincision factors are more stably bound to gapped (ssDNA gap-containing) NER intermediates. The higher concentration of RFCp140-GFP at LUD correlates with a higher concentration of substrate, i.e., gapped NER intermediates due to inhibition of DNA synthesis (8), to which this protein has affinity.

The exchange rate of (endogenous) RFC in the NER complex in the presence and absence of inhibitors was further analyzed in a competition experiment by applying a second

local damage infliction (with a different pore size) after the first irradiation in quiescent primary human cells. The cells were first irradiated locally with 30 J/m^2 of UVC through 8-μm pores. After 30 min of incubation to allow a maximum accumulation of NER complexes, the cells were again locally irradiated but this time through smaller pores (3 μm). Figure 6B (top panel) shows that in the absence of replication inhibitors, both TFIIH (p89) and RFCp140 were able to partially localize to the second LUD (of smaller pore size). However, in the presence of inhibitors, RFC was visible only at the initial damage site, similar to other postincision factors such as PCNA and RPA (Overmeer, unpublished); in contrast, p89 localizes to the second local damage site, similar to other preincision factors (data not shown). These data suggest that DNA synthesis factors remain associated or are continuously targeted to stalled postincision repair complexes. The underlying mechanism is that in the presence of inhibitors, no incisions are made at the second LUD site, and, hence, no substrate is created for these factors to bind to.

To further investigate whether DNA synthesis factors are stably associated or dynamically reassociate to stalled NER repair synthesis complexes, cells were submitted to FRAP analysis in LUD. We noticed that, in living cells (Fig. 6C), RFCp140-GFP exchanges from LUD after DNA synthesis inhibition, though with slower kinetics: ~50 s in untreated cells and ~70s in HU/Ara-C-treated cells for complete exchange at LUD. These data show that RFCp140 (and perhaps other replication factors) dynamically associates with and releases from stalled repair replication complexes. The absence of visible relocalization to the secondary LUD thus corroborates the hypothesis that repair synthesis inhibition prevents incisions at these secondary LUD sites in quiescent cells, preventing the creation of substrate for the postincision factors to bind. We conclude that the proteins are still exchanging and, therefore, behave in a more dynamic way than previously anticipated and that RFCp140 continues to be recruited to repair synthesis sites even after PCNA is loaded. The continued recruitment suggests an additional role beyond loading of the PCNA clamp.

DISCUSSION

Here, we have shown that RFC participates in NER *in vivo*, involving a highly dynamic association/dissociation cycle with NER intermediates. Previous studies (2, 4) revealed that purified RFC protein supported DNA repair synthesis *in vitro* employing a reconstituted NER system. The *in vitro* experiments show that purified RFC stimulates repair synthesis but does not unambiguously identify RFC as the actual clamp loader *in vivo*. For example, it was long thought that ligase I was the essential NER ligase as it was able to catalyze ligation in *in vitro* NER assays (2). Although we provided evidence for a role of ligase I in NER *in vivo*, in fact ligase III appears to be the dominant ligase in NER in living cells (32).

The role of RFC in NER *in vivo* is manifested by the reduced 6-4PP repair (Fig. 3) and repair synthesis (35) in cells with RFCp140 knockdown. These observations corroborate the previously described findings that impaired gap filling during postincision repair leads to reduced DNA damage removal (32, 34, 39). Moreover, the immunofluorescence analysis of endogenous RFC and the dynamic studies employing GFP-tagged RFCp140 provide direct evidence that RFC is recruited to sites of UV photolesions in an NER-dependent and cell cycle-independent fashion. Finally, the ChIP data show that RFC interacts with other postincision factors in nondividing human cells upon UV irradiation, consistent with its involvement in NER *in vivo*.

The function of RFC as clamp loader in replicative DNA synthesis is to open the trimeric PCNA ring to allow stable loading of the polymerase clamp at 3′ termini. Our live-cell protein dynamic studies favor such a role of RFC in NER: FRAP analysis of RFCp140-GFP showed that RFCp140-GFP dynamically dissociates and reassociates both with replication foci and LUD and that, on average, RFC molecules are bound to NER complexes for much shorter times than PCNA. These data are in line with a model according to which once RFC has loaded PCNA, the latter remains bound, and RFC leaves. However, other data (Fig. 3D and E) seem to challenge the role of RFC as the principal PCNA clamp-recruiting factor in NER. Most notably, whereas knockdown of RFCp140 reduced the recruitment of Polδ to less than 50% of colocalization, the PCNA recruitment was only mildly affected. These results lead to the unexpected conclusions that RFC is not required for the recruitment of PCNA to the postincision NER complex and that the association of PCNA with sites of damage is not sufficient to recruit other postincision factors such as Polδ. An obvious explanation is that PCNA gets recruited to sites of UV damage in an RFC-independent fashion but that this recruitment does not lead to a replication-competent form of PCNA; i.e., RFC is an essential factor required for stable loading of the polymerase clamp, which is necessary to start DNA repair synthesis. Stable loading is likely established by the ATPase activity of RFC that opens the PCNA ring and subsequently allows it to close when it is bound to the 3′ terminus generated by ERCC1-XPF incision (40).

The preincision factor p89 (TFIIH subunit) associates with secondary LUD (induced by sequential UV irradiation) when repair synthesis is inhibited (Fig. 6B). In contrast, endogenous RFC and PCNA are not loaded to secondary LUD sites, suggesting stable binding of the postincision NER factors to the initial LUD. The observed dynamic exchange of RFC on HU- and Ara-C-stalled repair replication (Fig. 6C) seems to contradict the results of immunofluorescence based competition experiments. However, in the immunofluorescence studies the complexes are frozen by the fixation and are thus not suited to reveal dynamic interactions. Stalled postincision repair complexes encompass incised DNA, all postincision factors, RPA, and an incomplete repair patch (34, 39; also Overmeer, unpublished) and obviously form a substrate to which RFC and PCNA dynamically interact with high affinity. We speculate that the RPA-coated 30-nt-long gapped NER intermediate generated by ERCC1-XPF-mediated 5′ incision (40) provides a high-affinity substrate for recruitment of both RFC and PCNA. Next, this intermediate allows preferential binding of RFC to the 3′ terminus and subsequent loading of PCNA. This dynamic mode of RFC association argues further that once PCNA is loaded, RFC dissociates and diffuses away from these sites. However, its localization at LUD long after damage induction, despite inhibition of incision, suggests a model in which RFCp140 continues to be recruited to the initial repair

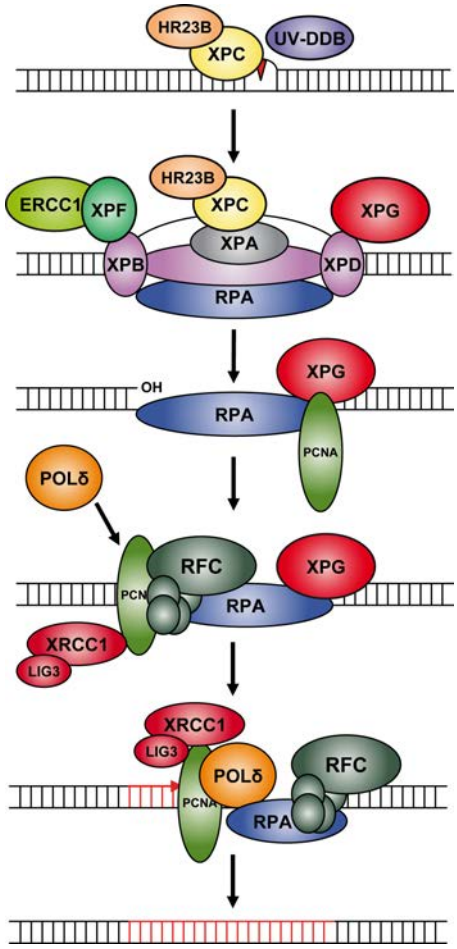

FIG. 7. Model of the NER process. After damage recognition by UV-DDB and/or XPC, the preincision complex is recruited, and the damage is verified. Next, the damage-containing oligonucleotide is excised by the XPF and XPG endonucleases, and preincision factors dissociate, with the exception of XPG and RPA. XPG and RPA are involved in the recruitment of PCNA and RFC, respectively, and subsequently PCNA can be loaded by RFC. After loading PCNA, RFC dissociates, and PCNA forms the sliding-clamp template required for the recruitment of other postincision factors. RFC is then able to bind the 5′ phosphate at the other side of the gap through its BRCT domain, where it possibly inhibits Rad17-dependent signaling or facilitates unloading of PCNA after completion of repair.

complex even after loading of PCNA. Hence, the dynamic interaction of RFC with sites of NER merely reflects a process of rapid dissociation/association of the complex with the RPA-coated gapped NER intermediate. Together, these data indicate that RFC displays additional functions beyond the clamp-loading activity, possibly functioning in subsequent binding of Polδ as described for *in vitro* replication of chromatin (48).

How is PCNA recruited into the postincision NER complex as immunofluorescence studies reveal that RFC is not required? *In vitro* experiments using reconstituted NER systems implicated XPG in the recruitment of PCNA to incised DNA (30), in line with earlier observations that XPG possesses PCNA binding capacity (12). In addition, impaired recruitment of PCNA is observed *in vivo* in XPG-deficient cells (9), whereas cells harboring a nuclease-dead mutant of XPG are still able to recruit PCNA (40). As XPF-deficient cells are unable to recruit PCNA, ERCC1-XPF-mediated 5′ incision might be required to allow XPG-dependent recruitment of PCNA. Based on this XPG-PCNA interaction, we propose a model in which PCNA is initially recruited by XPG, but only after incision is it positioned and loaded by RFC, which subsequently enables the recruitment of other postincision factors such as Polδ (Fig. 7) or any of the other DNA polymerases implicated in NER replication (35). Furthermore, our data are consistent with a model in which RFC exchanges dynamically to and from sites of repair even after loading PCNA, in contrast to earlier suggestions that RFC dissociates after PCNA loading to allow Polδ to bind (22, 37). The latter model is based on *in vitro* studies that employed an N-terminally truncated RFCp140 and therefore lacking a BRCT domain capable of binding 5′ phosphate (3, 26). We therefore speculate that RFC associates with the downstream 5′ phosphate after loading; such interaction would prevent possible signaling events initiated by Rad17 and may assist in unloading of PCNA (26). In model loading/unloading systems, human RFC has been shown to unload PCNA from template-primer DNA in an ATP-dependent reaction (47). Although the Ctf18-like complex is also capable of unloading PCNA (6), this seems more likely to occur during the establishment of sister chromatid cohesion. RFC would therefore represent a good candidate for performing this task in NER.

ACKNOWLEDGMENTS

We gratefully acknowledge B. Stillman and A. E. Tomkinson for kindly providing the anti-RFC p140 antibody and the anti-Lig1 antibody, respectively.

This work was supported by EU FP6 IP DNA Repair (LSHG-CT-2005-512113) and MRTN-CT-2003-503618, ZON-MW projects 912-03-012 and 917-46-364, ALW projects 805.3.42-P and 805.47.190 (MtC), and ESF projects ALW-855.01.074 and 805.47.193.

REFERENCES

1. **Abcam.** 2010. Nuclear fractionation protocol. Abcam Inc., Cambridge, MA. www.abcam.com/ps/pdf/protocols/Nuclear Fractionation protocol.pdf.
2. **Aboussekhra, A., M. Biggerstaff, M. K. K. Shivji, J. A. Vilpo, V. Moncollin, V. N. Podust, M. Protic, U. Hubscher, J. M. Egly, and R. D. Wood.** 1995. Mammalian DNA nucleotide excision repair reconstituted with purified protein components. Cell **80:**859–868.
3. **Allen, B. L., F. Uhlmann, L. K. Gaur, B. A. Mulder, K. L. Posey, L. B. Jones, and S. H. Hardin.** 1998. DNA recognition properties of the N-terminal DNA binding domain within the large subunit of replication factor C. Nucleic Acids Res. **26:**3877–3882.
4. **Araujo, S. J., F. Tirode, F. Coin, H. Pospiech, J. E. Syvaoja, M. Stucki, U. Hubscher, J. M. Egly, and R. D. Wood.** 2000. Nucleotide excision repair of DNA with recombinant human proteins: definition of the minimal set of factors, active forms of TFIIH, and modulation by CAK. Genes Dev. **14:** 349–359.
5. **Bermudez, V. P., L. A. Lindsey-Boltz, A. J. Cesare, Y. Maniwa, J. D. Griffith, J. Hurwitz, and A. Sancar.** 2003. Loading of the human 9-1-1 checkpoint complex onto DNA by the checkpoint clamp loader hRad17-replication factor C complex in vitro. Proc. Natl. Acad. Sci. U. S. A. **100:**1633–1638.
6. **Bylund, G. O., and P. M. Burgers.** 2005. Replication protein A-directed unloading of PCNA by the Ctf18 cohesion establishment complex. Mol. Cell. Biol. **25:**5445–5455.
7. **Ellison, V., and B. Stillman.** 2003. Biochemical characterization of DNA damage checkpoint complexes: Clamp loader and clamp complexes with specificity for 5′ recessed DNA. PLoS Biol. **1:**231–243.
8. **Erixon, K., and G. Ahnstrom.** 1979. Single-strand breaks in DNA during repair of UV-induced damage in normal human and xeroderma pigmentosum cells as determined by alkaline DNA unwinding and hydroxylapatite chromatography: effects of hydroxyurea, 5-fluorodeoxyuridine and 1-beta-D-arabinofuranosylcytosine on the kinetics of repair. Mutat. Res. **59:**257–271.
9. **Essers, J., A. F. Theil, C. Baldeyron, W. A. van Cappellen, A. B. Houtsmuller, R. Kanaar, and W. Vermeulen.** 2005. Nuclear dynamics of PCNA in DNA replication and repair. Mol. Cell. Biol. **25:**9350–9359.

10. **Fitch, M. E., S. Nakajima, A. Yasui, and J. M. Ford.** 2003. In vivo recruitment of XPC to UV-induced cyclobutane pyrimidine dimers by the DDB2 gene product. J. Biol. Chem. **278:**46906–46910.
11. **Fousteri, M., W. Vermeulen, A. A. van Zeeland, and L. H. F. Mullenders.** 2006. Cockayne syndrome A and B proteins differentially regulate recruitment of chromatin remodeling and repair factors to stalled RNA polymerase II in vivo. Mol. Cell **23:**471–482.
12. **Gary, R., D. L. Ludwig, H. L. Cornelius, M. A. MacInnes, and M. S. Park.** 1997. The DNA repair endonuclease XPG binds to proliferating cell nuclear antigen (PCNA) and shares sequence elements with the PCNA binding regions of FEN-1 and cyclin-dependent kinase inhibitor p21. J. Biol. Chem. **272:**24522–24529.
13. **Gerik, K. J., S. L. Gary, and P. M. Burgers.** 1997. Overproduction and affinity purification of *Saccharomyces cerevisiae* replication factor C. J. Biol. Chem. **272:**1256–1262.
14. **Gillet, L. C., and O. D. Scharer.** 2006. Molecular mechanisms of mammalian global genome nucleotide excision repair. Chem. Rev. **106:**253–276.
15. **Green, C. M., and G. Almouzni.** 2003. Local action of the chromatin assembly factor CAF-1 at sites of nucleotide excision repair in vivo. EMBO J. **22:**5163–5174.
16. **Hanawalt, P. C., and G. Spivak.** 2008. Transcription-coupled DNA repair: two decades of progress and surprises. Nat. Rev. Mol. Cell Biol. **9:**958–970.
17. **Hashiguchi, K., Y. Matsumoto, and A. Yasui.** 2007. Recruitment of DNA repair synthesis machinery to sites of DNA damage/repair in living human cells. Nucleic Acids Res. **35:**2913–2923.
18. **Hoeijmakers, J. H.** 2001. Genome maintenance mechanisms for preventing cancer. Nature **411:**366–374.
19. **Hoogstraten, D., S. Bergink, J. M. Ng, V. H. Verbiest, M. S. Luijsterburg, B. Geverts, A. Raams, C. Dinant, J. H. Hoeijmakers, W. Vermeulen, and A. B. Houtsmuller.** 2008. Versatile DNA damage detection by the global genome nucleotide excision repair protein XPC. J. Cell Sci. **121:**2850–2859.
20. **Houtsmuller, A. B.** 2005. Fluorescence recovery after photobleaching: application to nuclear proteins. Adv. Biochem. Eng. Biotechnol. **95:**177–199.
21. **Jaharul Haque, S., H. van der Kuip, A. Kumar, W. E. Aulitzky, M. N. Rutherford, C. Huber, T. Fischer, and B. R. Williams.** 1996. Overexpression of mouse p140 subunit of replication factor C accelerates cellular proliferation. Cell Growth Differ. **7:**319–326.
22. **Johnson, A., N. Y. Yao, G. D. Bowman, J. Kuriyan, and M. O'Donnell.** 2006. The replication factor C clamp loader requires arginine finger sensors to drive DNA binding and proliferating cell nuclear antigen loading. J. Biol. Chem. **281:**35531–35543.
23. **Kanellis, P., R. Agyei, and D. Durocher.** 2003. Elg1 forms an alternative PCNA-interacting RFC complex required to maintain genome stability. Curr. Biol. **13:**1583–1595.
24. **Kim, J., and S. A. MacNeill.** 2003. Genome stability: a new member of the RFC family. Curr. Biol. **13:**R873–R875.
25. **Kim, J., K. Robertson, K. J. Mylonas, F. C. Gray, I. Charapitsa, and S. A. MacNeill.** 2005. Contrasting effects of Elg1-RFC and Ctf18-RFC inactivation in the absence of fully functional RFC in fission yeast. Nucleic Acids Res. **33:**4078–4089.
26. **Kobayashi, M., F. Figaroa, N. Meeuwenoord, L. E. T. Jansen, and G. Siegal.** 2006. Characterization of the DNA binding and structural properties of the BRCT region of human replication factor C p140 subunit. J. Biol. Chem. **281:**4308–4317.
27. **Kraemer, K. H., N. J. Patronas, R. Schiffmann, B. P. Brooks, D. Tamura, and J. J. DiGiovanna.** 2007. Xeroderma pigmentosum, trichothiodystrophy and Cockayne syndrome: a complex genotype-phenotype relationship. Neuroscience **145:**1388–1396.
28. **Leonhardt, H., H. P. Rahn, P. Weinzierl, A. Sporbert, T. Cremer, D. Zink, and M. C. Cardoso.** 2000. Dynamics of DNA replication factories in living cells. J. Cell Biol. **149:**271–280.
29. **Luijsterburg, M. S., B. G. von, A. M. Gourdin, A. Z. Politi, M. J. Mone, D. O. Warmerdam, J. Goedhart, W. Vermeulen, D. R. van, and T. Hofer.** 2010. Stochastic and reversible assembly of a multiprotein DNA repair complex ensures accurate target site recognition and efficient repair. J. Cell Biol. **189:**445–463.
30. **Mocquet, V., J. P. Laine, T. Riedl, Z. Yajin, M. Y. Lee, and J. M. Egly.** 2008. Sequential recruitment of the repair factors during NER: the role of XPG in initiating the resynthesis step. EMBO J. **27:**155–167.
31. **Moné, M. J., M. Volker, O. Nikaido, L. H. F. Mullenders, A. A. van Zeeland, P. J. Verschure, E. M. M. Manders, and R. van Driel.** 2001. Local UV induced DNA damage in cell nuclei results in local transcription inhibition. EMBO Rep. **2:**1013–1017.
32. **Moser, J., H. Kool, I. Giakzidis, K. Caldecott, L. H. F. Mullenders, and M. I. Fousteri.** 2007. Sealing of chromosomal DNA nicks during nucleotide excision repair requires XRCC1 and DNA ligase III alpha in a cell-cycle-specific manner. Mol. Cell **27:**311–323.
33. **Moser, J., M. Volker, H. Kool, S. Alekseev, H. Vrieling, A. Yasui, A. A. van Zeeland, and L. H. F. Mullenders.** 2005. The UV-damaged DNA binding protein mediates efficient targeting of the nucleotide excision repair complex to UV-induced photo lesions. DNA Repair (Amst.) **4:**571–582.
34. **Mullenders, L. H. F., A. C. Vankesterenvanleeuwen, A. A. Vanzeeland, and A. T. Natarajan.** 1985. Analysis of the structure and spatial-distribution of ultraviolet-induced DNA repair patches in human cells made in the presence of inhibitors of replicative synthesis. Biochim. Biophys. Acta **826:**38–48.
35. **Ogi, T., S. limsirichaikul, R. M. Overmeer, M. Volker, K. Takenaka, R. Cloney, Y. Nakazawa, A. Niimi, Y. Miki, N. G. Jaspers, L. H. Mullenders, S. Yamashita, M. I. Fousteri, and A. R. Lehmann.** 2010. Three DNA polymerases, recruited by different mechanisms, carry out NER repair synthesis in human cells. Mol. Cell **37:**714–727.
36. **Parrilla-Castellar, E. R., S. J. Arlander, and L. Karnitz.** 2004. Dial 9-1-1 for DNA damage: the Rad9-Hus1-Rad1 (9-1-1) clamp complex. DNA Repair (Amst.) **3:**1009–1014.
37. **Podust, V. N., N. Tiwari, S. Stephan, and E. Fanning.** 1998. Replication factor C disengages from proliferating cell nuclear antigen (PCNA) upon sliding clamp formation, and PCNA itself tethers DNA polymerase delta to DNA. J. Biol. Chem. **273:**31992–31999.
38. **Shiomi, Y., A. Shinozaki, K. Sugimoto, J. Usukura, C. Obuse, and T. Tsurimoto.** 2004. The reconstituted human Chl12-RFC complex functions as a second PCNA loader. Genes Cells **9:**279–290.
39. **Smith, C. A., and D. S. Okumoto.** 1984. Nature of DNA repair synthesis resistant to inhibitors of polymerase-alpha in human-cells. Biochemistry **23:**1383–1391.
40. **Staresincic, L., A. F. Fagbemi, J. H. Enzlin, A. M. Gourdin, N. Wijgers, I. Dunand-Sauthier, G. Giglia-Mari, S. G. Clarkson, W. Vermeulen, and O. D. Scharer.** 2009. Coordination of dual incision and repair synthesis in human nucleotide excision repair. EMBO J. **28:**1111–1120.
41. **Tsurimoto, T., and B. Stillman.** 1989. Purification of a cellular replication factor, RF-C, that is required for coordinated synthesis of leading and lagging strands during simian virus 40 DNA replication in vitro. Mol. Cell. Biol. **9:**609–619.
42. **van den Boom, V., E. Citterio, D. Hoogstraten, A. Zotter, J. M. Egly, W. A. van Cappellen, J. H. Hoeijmakers, A. B. Houtsmuller, and W. Vermeulen.** 2004. DNA damage stabilizes interaction of CSB with the transcription elongation machinery. J. Cell Biol. **166:**27–36.
43. **van der Kuip, H., B. Carius, S. J. Haque, B. R. Williams, C. Huber, and T. Fischer.** 1999. The DNA-binding subunit p140 of replication factor C is upregulated in cycling cells and associates with G_1 phase cell cycle regulatory proteins. J. Mol. Med. **77:**386–392.
44. **van Hoffen, A., J. Venema, R. Meschini, A. A. van Zeeland, and L. H. Mullenders.** 1995. Transcription-coupled repair removes both cyclobutane pyrimidine dimers and 6-4 photoproducts with equal efficiency and in a sequential way from transcribed DNA in xeroderma pigmentosum group C fibroblasts. EMBO J. **14:**360–367.
45. **Volker, M., M. J. Mone, P. Karmakar, A. van Hoffen, W. Schul, W. Vermeulen, J. H. J. Hoeijmakers, R. van Driel, A. A. van Zeeland, and L. H. F. Mullenders.** 2001. Sequential assembly of the nucleotide excision repair factors in vivo. Mol. Cell **8:**213–224.
46. **Waga, S., and B. Stillman.** 1998. The DNA replication fork in eukaryotic cells. Annu. Rev. Biochem. **67:**721–751.
47. **Yao, N., J. Turner, Z. Kelman, P. T. Stukenberg, F. Dean, D. Shechter, Z. Q. Pan, J. Hurwitz, and M. O'Donnell.** 1996. Clamp loading, unloading and intrinsic stability of the PCNA, beta and gp45 sliding clamps of human, *E. coli* and T4 replicases. Genes Cells **1:**101–113.
48. **Yuzhakov, A., Z. Kelman, J. Hurwitz, and M. O'Donnell.** 1999. Multiple competition reactions for RPA order the assembly of the DNA polymerase delta holoenzyme. EMBO J. **18:**6189–6199.